Relationship Between Sulfide Capacity and Structure of $MnO-SiO_2-Al_2O_3-Ce_2O_3$ System

SE JI JEONG, TAE SUNG KIM, and JOO HYUN PARK

Sulfide capacity of the $MnO-SiO_2-Al_2O_3-Ce_2O_3$ system was measured at 1873 K (1600 °C), and the structural analysis was carried out using micro-Raman spectroscopy to understand the role of Ce_2O_3 in the sulfur dissolution behavior. Sulfide capacity of the basic melts ($MnO/SiO_2 = 2.2(\pm 0.14)$) decreased with increasing content of Ce_2O_3 to approx. 4 mol pct, beyond which it increased. Sulfide capacity continuously decreased in the less basic system ($MnO/SiO_2 = 1.0(\pm 0.15)$), whereas it was hardly affected by Ce_2O_3 in the relatively acidic composition ($MnO/SiO_2 = 0.3(\pm 0.05)$). There was a significant increase in the intensity of Raman band at 600 cm^{-1} by Ce_2O_3 addition in high MnO/SiO_2 (= 2.2) system, which originated from the transition from $[(Al,Mn_{0.5})O_4]$-tetrahedron to $[(Al,Ce)O_6]$-octahedron due to strong attraction between Al_2O_3 and Ce_2O_3. Combining thermodynamic and structural information, the effect of Ce_2O_3 on the sulfide capacity of Mn-aluminosilicate melts can be explained by the following factors: (1) Activity of MnO in the melts decreased by addition of Ce_2O_3; (2) Free oxygen was consumed in the structure modification from $[(Al,Mn_{0.5})O_4]$ to $[(Al,Ce)O_6]$ unit by addition of Ce_2O_3; and 3) When the Ce^{3+} content was greater than critical value (approx. 4 mol pct) in high MnO/SiO_2 (= 2.54) melts, excess Ce^{3+} and Mn^{2+} ions competitively reacted with S^{2-} ions, resulting in an increase of sulfide capacity.

DOI: 10.1007/s11663-016-0828-1

I. INTRODUCTION

It is well known that sulfur is harmful to the mechanical properties of steel product such as strength, ductility, toughness. Also, sulfide or oxy-sulfide inclusions deteriorate the corrosion resistance and oxidation resistance of stainless steels, and thus it is desirable that these harmful inclusions should be effectively removed.[1,2] However, sulfur is contained as an impurity in various alloying materials such as ferroalloys. The formation of rare earth sulfide or oxy-sulfide inclusions in molten steel is unavoidable due to high affinity between rare earth elements and sulfur at steelmaking temperatures. Therefore, the sulfur absorption ability of the oxide system containing rare earth elements should be necessarily investigated at high temperatures.

Recently, Kwon *et al.*[3,4] investigated the thermodynamic behavior of Ce in austenitic stainless steel melts in terms of Ce yield and inclusion evolution procedure as well as interfacial reaction between alumina refractory and molten steel. Looking at the behavior of the inclusions, the Mn(Cr)-silicate inclusions were initially formed, followed by a transformation to the $MnO-SiO_2-Al_2O_3$ ternary system by an Al deoxidation. Finally, the $MnO-SiO_2-Al_2O_3-CeO_X$ complex oxides were partly formed after Ce was added, which was well agreed to the results observed by Jeon *et al.*[1,2] Therefore, the sulfide capacity of the $MnO-SiO_2-Al_2O_3-CeO_X$ melt needs to be measured to figure out the sulfur absorption ability of this quaternary oxide system.

The sulfide capacity of the $MnO-SiO_2-Al_2O_3$ ternary system is well known from the previous articles.[5–7] Sharma and Richardson described the iso-sulfide capacity contours from the measured capacity results at the compositions of $X_{SiO_2} \le 0.5$ and $X_{MnO} \le 0.8$ using gas-slag equilibration method at 1923 K (1650 °C).[5] Nzotta calculated the iso-sulfide capacity contours using the mathematical model at 1873 K (1600 °C), and the model predictions were agreed well with the measured results in the composition ranges of $0.3 \le X_{SiO_2} \le 0.6$ and $0.3 \le X_{MnO} \le 0.6$.[6] Recently, Kang and Pelton calculated the iso-sulfide capacity contours in the $MnO-SiO_2-Al_2O_3$ system using the modified quasichemical model based on the quadruplet approximation at 1923 K (1650 °C) and compared the calculated results with the experimental data measured by Sharma and Richardson.[7] From these previous results, it is generally known that the sulfide capacity increases with increasing content of MnO in the $MnO-SiO_2-Al_2O_3$ ternary system.

On the other hand, the activity of each component in the $MnO-SiO_2-Al_2O_3$ system is of essential importance in evaluation of sulfide capacity. Woo *et al.*[8] reported the iso-a_{MnO} contours in the $MnO-SiO_2-Al_2O_3$ system using the quadric formalism at 1823 K (1550 °C) by

SE JI JEONG, formerly Graduate Student with the Department of Materials Engineering, Hanyang University, Ansan, 426-791, Korea, is now Researcher with Technical Research Center, SeAH Changwon Integrated Specialty Steel (SeAH CSS), Changwon, Korea. TAE SUNG KIM, Graduate Student, and JOO HYUN PARK, Professor, are with the Department of Materials Engineering, Hanyang University. Contact e-mail: basicity@hanyang.ac.kr

Manuscript submitted July 28, 2016.
Article published online October 12, 2016.

equilibrating the MnO-SiO_2-Al_2O_3 melts of different compositions with the Pt-Mn alloys, from which it is known that the activity of MnO is strongly dependent on the mole fraction of MnO and SiO_2 rather than that of Al_2O_3. These tendencies are also found in Ohta and Suito,[9] and Fujisawa and Sakao's works.[10]

Anacleto *et al.*[11] measured the sulfur partition ratio (L_S) between CaO-SiO_2-Ce_2O_3 slag and carbon-saturated iron at 1773 K (1500 °C) and found that L_S increased with increasing amount of Ce_2O_3 in the slag. They tentatively concluded that Ce_2O_3 decreased the activity coefficient of SiO_2 in the CaO-SiO_2-Ce_2O_3 slag. However, they did not provide any clear thermodynamic analysis for the increase in L_S by increasing the content of Ce_2O_3. Furthermore, there is no experimental study on the sulfide capacity of manganese aluminosilicate melts containing cerium oxide. Consequently, in the present study, we measured the sulfide capacity of the MnO-SiO_2-Al_2O_3-Ce_2O_3 quaternary system by gas-slag equilibration method at 1873 K (1600 °C), and the structural analysis was also carried out using micro-Raman spectroscopic method to understand the role of Ce_2O_3 in the sulfur dissolution behavior in the present oxide system because none of thermodynamic information (activity of each component, phase equilibria, *etc.*) of the MnO-SiO_2-Al_2O_3-Ce_2O_3 system is available.

II. EXPERIMENTAL

A super-kanthal vertical electric furnace was used for the equilibration between the MnO-SiO_2-Al_2O_3-Ce_2O_3 melt and gas phase at 1873 K (1600 °C). The temperature was controlled within ±2 K (±2 °C) using an installed B-type (Pt-30Rh/Pt-6Rh, mass pct) thermocouple and a proportional integral differential controller. The furnace temperature was also calibrated using an external B-type thermocouple before experiment. As shown in Figure 1, the effect of Ce oxide on sulfide capacity was evaluated by adding reagent-grade CeO_2 at marked composition A (66(±2) mol pct SiO_2), B (43(±2) mol pct SiO_2), and C (26(±1) mol pct SiO_2) at fixed alumina content (14(±1) mol pct) in the MnO-SiO_2-Al_2O_3 phase diagram.

The slag samples were prepared using reagent-grade MnO, SiO_2, Al_2O_3, and CeO_2. The slag sample of 1.2 g was maintained in a platinum crucible which was held in the porous alumina holder under the CO-CO_2-SO_2-Ar gas mixture for 12 hours. A constant flow rate of 400 mL/min was maintained during the equilibration of the slag with gas mixture at the experimental temperature. The schematic diagram of the experimental apparatus is shown in Figure 2. Each gas was passed through the purification system to remove the impurities. The flow rate of each gas and the calculated oxygen and sulfur potentials are listed in Table I. The more detailed experimental conditions and procedure are available in our previous articles.[12–14]

After equilibration, the sample was quickly drawn from the furnace and then quenched by dipping it into brine. The quenched samples were crushed to less than 100 μm using crusher for chemical analysis. The content

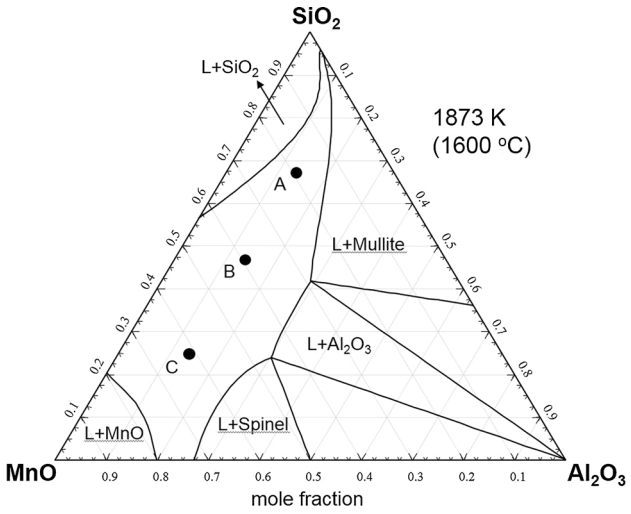

Fig. 1—Experimental composition in the MnO-SiO_2-Al_2O_3 phase diagram at 1873 K (1600 °C) (calculated using FactSage™7.0).

of sulfur and each component in the slag were determined by combustion analyzer (LECO, CS-250) and X-ray fluorescence spectroscopy (XRF, Bruker, S4 Explorer), respectively. The experimental compositions and the results are listed in Table II. All the samples were sent to X-ray diffraction (XRD) analysis to confirm the samples were glassy (amorphous) state.

The spectra for the binding energy of Ce3d were measured using an X-ray photoelectron spectroscopy analyzer (XPS, K-alpha by Thermo UK) in order to confirm the electronic state of Ce in the quenched glass samples. A monochromatized Al-Kα radiation (1486.6 eV) was used as the X-ray source, which was operated at 3 mA and 12 kV. The rod shaped samples were fractured in ultrahigh vacuum (4.8×10^{-7} Pa). The surface charging was neutralized by flooding electrons. In order to correct the charging effects, the measured binding energies were calibrated using the binding energy of the adventitious C1s line assuming that the C1s core level is 284.6 eV.

Finally, the micro-Raman spectroscopic analysis was carried out using a 'LabRamAramis' Horiba JobinYvon spectrometer. The 514 nm line of an Ar-ion laser was used for the measurements of Raman scattering of the quenched glass samples. The more details for the preparation, measurement procedure, and data processing are available in our previous articles.[15–17]

III. RESULTS AND DISCUSSION

A. *Predominant Ionic Speciation of Cerium in MnO-SiO_2-Al_2O_3-CeO_x System*

In general, the most of rare earth oxides are stable as sesquioxides ($[M^{3+}]_2[O^{2-}]_3$), nonetheless, cerium oxide is stable as CeO_2 at room temperature and oxygen enriched atmosphere. However, it is known to be reduced to Ce_2O_3 under reducing atmosphere.[18] Thus, it is important to investigate the stable ionic speciation of Ce in the Mn-aluminosilicate melts under the present

experimental conditions to understand the interaction between Ce^{n+}-O^{2-} and Ce^{n+}-S^{2-} pairs in structural view. Here, we employed the spectroscopic analysis (*via* XPS) to confirm the ionic state of Ce in the present system as follows.

A-Rivera *et al.*[19] and Sekita *et al.*[20] have confirmed trivalent cerium from XPS analysis in oxide glasses. Similarly, it was also confirmed that cerium mainly exists as Ce^{3+} in the Mn-aluminosilicate system as shown in Figure 3. Makishima *et al.*[21] observed that Ce^{3+}/Ce^{4+} ratio in the Ce-containing aluminosilicate glass prepared at 1823 K (1600 °C) for 3h in air was 89/11 from wet chemical analysis. Even though there is a small peak at 916 eV (corresponds to Ce^{4+}) in Figure 4, the relative intensity of Ce^{3+} peaks (886.4 and 904.3 eV) is much greater than that of Ce^{4+}. Therefore, it is confirmed that the cerium is stabilized as Ce^{3+} in the Mn-aluminosilicate system under the relatively reducing atmosphere at 1873 K (1600 °C).

B. *Effect of Ce_2O_3 on Sulfide Capacity of MnO-SiO_2-Al_2O_3-Ce_2O_3 System*

Sulfide capacity ($C_{S^{2-}}$) of the molten slag was originally defined by Finchan and Richardson as given in Eq. [2] deduced from the desulfurization reaction (Eq. [1]) based on a slag-gas equilibrium.[22]

$$\frac{1}{2}S_2(g) + (O^{2-}) = (S^{2-}) + \frac{1}{2}O_2(g), \qquad [1]$$

$$C_{S^{2-}} \equiv \frac{K_{[1]} \cdot a_{O^{2-}}}{f_{S^{2-}}} = (\text{mass pct } S^{2-}) \cdot \left(\frac{p_{O_2}}{p_{S_2}}\right)^{\frac{1}{2}}, \qquad [2]$$

where $K_{(1)}$: equilibrium constant of Eq. [1], $a_{O^{2-}}$: activity of O^{2-} ion in slag (=basicity of slag), $f_{S^{2-}}$: activity coefficient of sulfide ion (S^{2-}) in slag, p_i: partial pressure of gaseous component i, atm.

From Eq. [2], the sulfide capacity is known to be a function of basicity, the stability of sulfide ion in molten slag, and temperature. Thus, it is a unique function of melt composition at a given temperature and can be experimentally determined from the sulfur content, and gaseous oxygen and sulfur potentials.

The effect of MnO on the sulfide capacity of the MnO-SiO_2-Al_2O_3 ($X_{Al_2O_3} = 0.15$) system at 1873 K (1600 °C) is shown in Figure 4, wherein the experimental results measured by Sharma and Richardson [at 1923 K (1650 °C)], and Nzotta [at 1873 K (1600 °C)] are also compared.[5,6] The sulfide capacity of the MnO-SiO_2-Al_2O_3 ($X_{Al_2O_3} = 0.15$) system increase with increasing content of MnO, *i.e.*, MnO/SiO_2 ratio, indicating that the MnO behaves as a basic oxide which directly contributes to an increase in basicity ($a_{O^{2-}}$) of the aluminosilicate melts based on Eq. [3].[12–14] This tendency is in good agreement with the

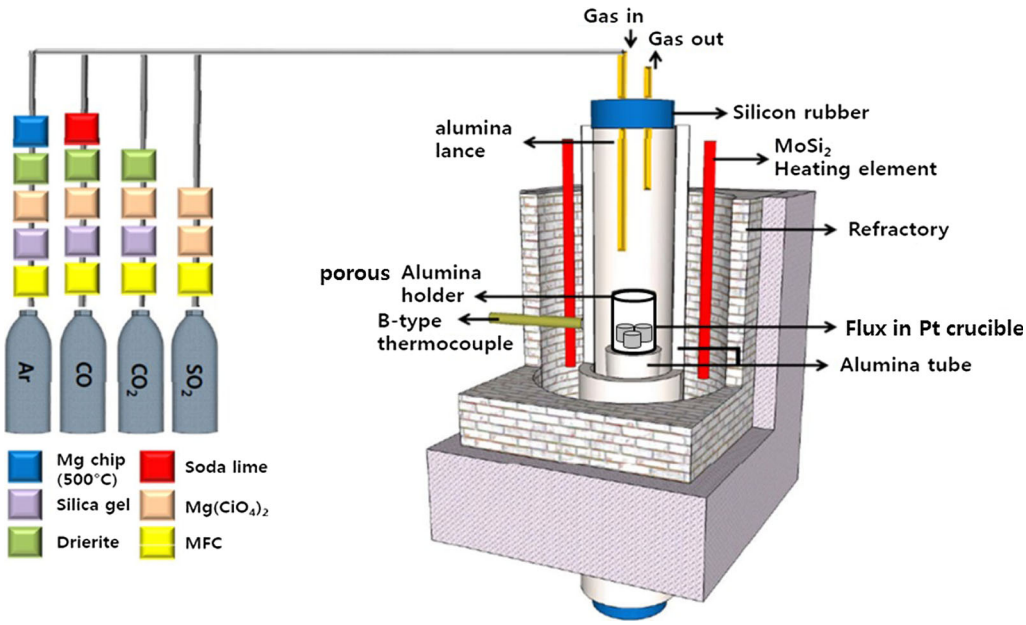

Fig. 2—Schematic diagram of the experimental apparatus.

Table I. Mass Flow of Each Gas and Calculated Oxygen and Sulfur Partial Pressure

Mass Flow of Gas Phases (mL/min)					Gas Potential (atm)	
CO	CO_2	SO_2	Ar	Total	$p(O_2)$	$p(S_2)$
125	160	15	100	400	2.8×10^{-7}	4.7×10^{-3}

Table II. Experimental Compositions and Sulfide Capacities of the Slags

Mol Pct MnO	Mol Pct SiO_2	Mol Pct Al_2O_3	Mol Pct Ce_2O_3	Mass Pct S	log C_S
57.4	26.6	16.0	0.0	1.701	−1.88
57.8	26.2	14.8	1.2	0.333	−2.59
58.7	23.6	15.1	2.7	0.298	−2.64
54.4	26.5	15.4	3.7	0.254	−2.71
55.1	24.8	14.5	5.6	0.582	−2.35
40.6	44.9	14.5	0.0	0.142	−2.96
45.0	40.9	13.0	1.1	0.156	−2.91
46.5	39.5	11.6	2.4	0.096	−3.13
36.3	46.1	14.0	3.6	0.074	−3.24
37.5	44.3	13.1	5.0	0.077	−3.22
21.3	65.0	13.7	0.0	0.016	−3.91
16.1	68.9	14.0	0.9	0.012	−4.01
22.1	62.6	13.1	2.3	0.011	−4.06
15.0	68.4	13.7	2.9	0.016	−3.90
19.2	62.9	13.3	4.6	0.012	−4.01

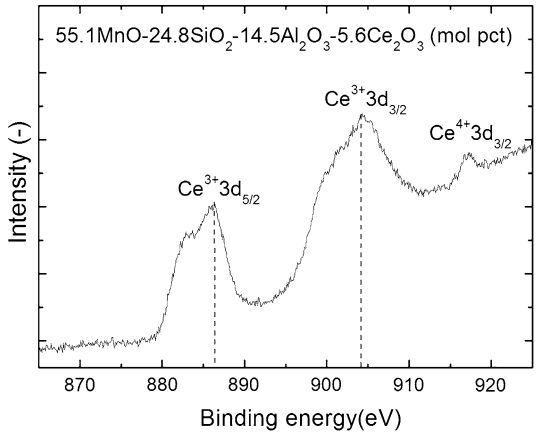

Fig. 3—The Ce 3d photoemission core level spectra of the quenched glass sample showing the spin-orbit doublet Ce $3d_{3/2}$ and Ce $3d_{5/2}$.

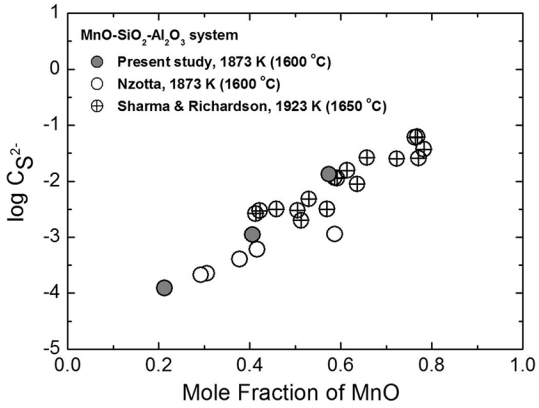

Fig. 4—Effect of MnO content on the sulfide capacity of the MnO-SiO_2-Al_2O_3 system.

literature data even though there are some experimental scatters.

$$(\mathrm{MnO}) = \left(\mathrm{Mn}^{2+}\right) + \left(\mathrm{O}^{2-}\right), \qquad [3]$$

The effect of Ce_2O_3 on the sulfide capacity of the MnO-SiO_2-Al_2O_3-Ce_2O_3 system ($X_{MnO}/X_{SiO_2} = 0.3$ ($\pm$0.05),1.0($\pm$0.15),2.2($\pm$0.14)) at 1873 K (1600 °C) is shown in Figure 5. It is very interesting that the influence of Ce_2O_3 on the sulfide capacity exhibits a different tendency according to the MnO/SiO_2 (= M/S) ratio. The sulfide capacity of the oxide melts with highly basic composition, *i.e.*, M/S = 2.2, decreases with increasing content of Ce_2O_3 to approx. 4 mol pct, beyond which the sulfide capacity increases by increasing the Ce_2O_3 content. The sulfide capacity continuously decreases as the Ce_2O_3 is added to the Mn-aluminosilicate melts in the less basic system, *i.e.*, M/S = 1.0, whereas it is hardly affected by Ce_2O_3 in the relatively acidic (high silica) composition, *i.e.*, M/S = 0.3.

Therefore, it is not easy to explain these complicated phenomena in regard of the role of Ce_2O_3 in the sulfur dissolution into the Mn-aluminosilicate melts using simple terminology, *e.g.*, basic, acidic, and amphoteric behavior of Ce_2O_3. Actually, Ce_2O_3 can be considered as an amphoteric oxide based on the ion-oxygen attraction (I_{MO}) parameter calculated from coulombic force between cation and oxygen, *i.e.*, $I_{MnO} = 0.83$, $I_{Ce_2O_3} = 1.03$, $I_{Al_2O_3} = 1.66$, and $I_{SiO_2} = 2.44$,[23] indicating that Ce_2O_3 is less basic than MnO and is more basic than Al_2O_3 and SiO_2. Hence, the more systematic discussions are needed to understand the effect of Ce_2O_3 on sulfide capacity of the MnO-SiO_2-Al_2O_3-Ce_2O_3 system based on the relationship between thermodynamic and structural properties.

It is known that the affinity between Ce^{3+} and S^{2-} is greater than that of Mn^{2+} and S^{2-} in view of the Gibbs free energy of the formation of Ce_2S_3 and MnS based on Eqs. [4] and [5].[24,25]

$$\mathrm{MnO(s)} + \frac{1}{2}\mathrm{S_2(g)} = \mathrm{MnS(s)} + \frac{1}{2}\mathrm{O_2(g)}, \qquad [4]$$
$$\Delta G^{\circ} = 93,190\ \mathrm{(J/mol)\ at\ 1873\ K},$$

$$\mathrm{Ce_2O_3(s)} + \frac{3}{2}\mathrm{S_2(g)} = \mathrm{Ce_2S_3(s)} + \frac{3}{2}\mathrm{O_2(g)}, \qquad [5]$$
$$\Delta G^{\circ} = 22,273\ \mathrm{(J/mol)\ at\ 1873\ K}.$$

Also, it can be reasonably assumed that the basicity of the MnO-SiO_2-Al_2O_3-Ce_2O_3 system is dominantly

affected by the activity of MnO as mentioned above (in Figure 4 and Eq. [3]). From the iso-activity contours of MnO in the $MnO-SiO_2-Al_2O_3$ system at 1823 K (1550 °C) measured by Woo *et al.*,[8] the MnO activity strongly depends on the MnO content, *i.e.*, MnO/SiO_2 ratio as shown in Figure 6, and it is less sensitive to the Al_2O_3 content. In the viewpoint of thermodynamics, this means that MnO preferentially interacts with SiO_2 in Mn-aluminosilicate melts. When the mole fraction of MnO exceeds about 0.5, the activity of MnO decreases very rapidly by decreasing the concentration of MnO.

In the present $MnO-SiO_2-Al_2O_3-Ce_2O_3$ system, the concentration of MnO becomes slightly diluted as Ce_2O_3 is added, by which the activity of MnO decreases. A decreasing rate of MnO activity due to MnO dilution is more significant at higher MnO region, *i.e.*, M/S = 2.2 than that of the lower MnO regions, *i.e.*, M/S = 0.3-1.0 at fixed temperature. Therefore, it is qualitatively concluded that the basicity of the oxide melts decreased by addition of Ce_2O_3, resulting in a decrease of sulfide capacity, and this tendency is more significant in the more basic composition regions as shown in Figure 5.

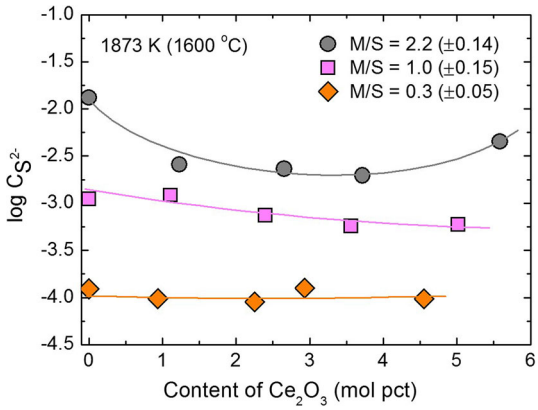

Fig. 5—Effect of Ce_2O_3 on the sulfide capacity of the $MnO-SiO_2-Al_2O_3-Ce_2O_3$ system with different MnO/SiO_2 ratios at 1873 K (1600 °C).

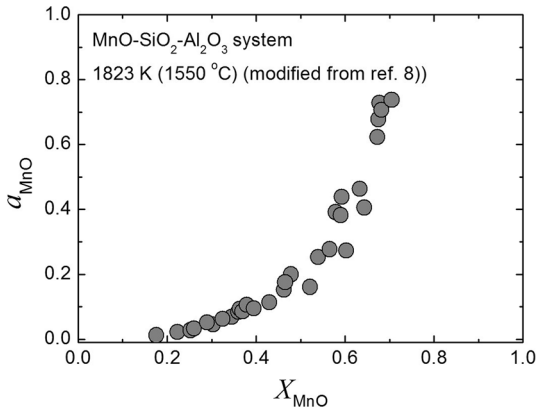

Fig. 6—Dependence of MnO activity on the content of MnO in the $MnO-SiO_2-Al_2O_3$ ternary system at 1823 K (1550 °C) (modified from Ref. [8]).

However, in Figure 5, the sulfide capacity of the basic system (M/S = 2.2) rebounds at Ce_2O_3 content greater than about 4 mol pct, which cannot be simply explained by the dilution effect of MnO. In order to thermodynamically understand these complicated phenomena, both the activity coefficient of MnS (or Ce_2S_3) and the activity of MnO (or Ce_2O_3) should be evaluated. However, unfortunately, because none of thermodynamic data (activity of each component, phase equilibria, *etc.*) of the $MnO-SiO_2-Al_2O_3-Ce_2O_3$ system is available in the literature (actually, thermodynamic databases for the $MnO-SiO_2-Al_2O_3$ ternary and $Ce_2O_3-Al_2O_3$ binary subsystems are available in FactSage™ software and related literatures), the Raman spectroscopic analyses for the influence of Ce_2O_3 on the ionic structure of Mn-aluminosilicate system was employed in the present study to reveal the *Composition-Structure-Property* relationship.

C. *Structural Behavior of Ce^{3+} Ions in Aluminosilicate Melts*

In the viewpoint of the structural role of cations in oxide melts and glasses, the role of cations is primarily determined by the size and charge (*i.e.*, ionic potential) of them in the networks.[14–17,26] According to Lin *et al.*,[26] because Ce^{3+} ion (r = 1.01 Å) has a radius close to that of Ca^{2+} (r = 1.0 Å) or Na^{+} (r = 1.02 Å), it is too large to be a (tetrahedrally coordinated) network former like $[SiO_4]$ or $[AlO_4]$ units. Therefore, they suggested that the Ce^{3+} conducts a role of charge compensator or network modifier rather than network former. Wu and Pelton reported the strong affinity between Ce_2O_3 and Al_2O_3 through the coupled thermodynamic-phase diagram analysis in order to refine the assessments of thermodynamic properties of $R_2O_3-Al_2O_3$ (R; Rare earth) binary systems.[27] Morita *et al.*[28,29] found that the addition of Ce_2O_3 to the $CaO-Al_2O_3$ system at 1773 K (1500 °C) decreases the activity coefficient of Al_2O_3 in the melts because of the strong attraction between Ce_2O_3 and Al_2O_3 based on the following reaction.

$$CeO_{1.5}(s) + AlO_{1.5}(s) = CeO_{1.5} \cdot AlO_{1.5}(s), \quad \Delta G^{o} = -58,730(\text{J/mol}) \text{ at } 1873\text{ K}. \qquad [6]$$

Hence, there is a strong attractive force between Ce_2O_3 and Al_2O_3 in the present Mn-aluminosilicate system. In the viewpoint of the amphoteric behavior of alumina in the aluminosilicate melts,[30,31] the aluminate anion will exist as $[AlO_4]$-tetrahedron, which is balanced with the half mole of Mn^{2+} cations (expressed as hypothetical $[(Al,Mn_{0.5})O_4]$-unit as similar as $[SiO_4]$-unit) as schematically shown in Figure 7(a). However, when the Ce_2O_3 is added, the $[AlO_6]$-octahedron becomes more stable than $[AlO_4]$-tetrahedral unit due to high attractive force between Ce^{3+} and $[AlO_n]$-units,[26] resulting in the formation of hypothetical $[(Al,Ce)O_6]$-unit, as shown in Figure 7(b). It is expressed by the following Eq. [7].

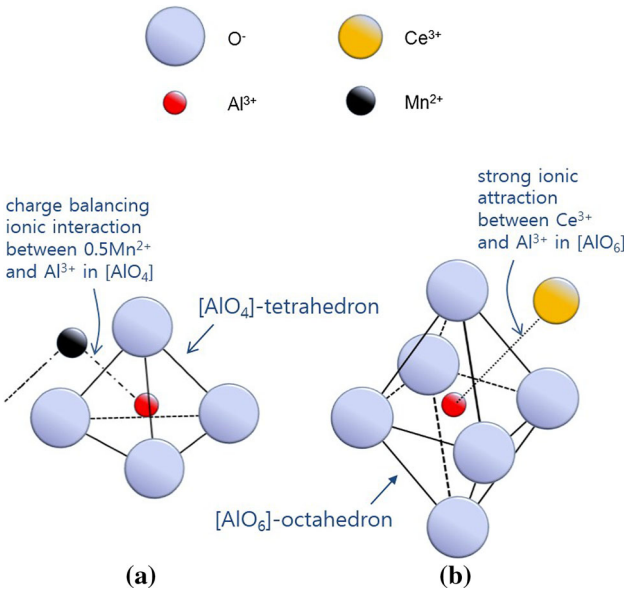

Fig. 7—Schematics of the ionic structure of (*a*) $[AlO_4]$-tetrahedron balanced with $0.5Mn^{2+}$ ion (hypothetically shown as $[(Al, Mn_{0.5})O_4]$-unit) and (*b*) $[AlO_6]$-octahedron balanced with Ce^{3+} ion (hypothetically shown as $[(Al,Ce)O_6]$-unit).

$$[(Al, Mn_{0.5})O_4]^{4-} + Ce^{3+} + 2O^{2-} = [(Al, Ce)O_6]^{6-} + 0.5Mn^{2+}. \quad [7]$$

From the above reaction, the free oxygen is employed to form $[(Al,Ce)O_6]$-unit. According to the previous researchers,[26–29] the addition of Ce_2O_3 to the aluminate or aluminosilicate melts promotes the network depolymerization and decreases the activity of alumina. Based on these thermodynamic (activity) and structural information, the *Composition-Structure-Capacity* relationship will be discussed in the following section.

D. *Effect of Ce_2O_3 on Sulfide Capacity of MnO-SiO_2-Al_2O_3-Ce_2O_3 System; Structural Understanding by Raman Spectroscopy*

Park *et al.*[12–17] recently investigated the relationship between structure and sulfide capacity of aluminosilicate melts containing calcium and manganese oxides. Because the sulfide capacity is function of basicity and stability of sulfide ion in aluminosilicate melts at fixed temperature, we considered that the activity of O^{2-} (basicity) and the activity coefficient of S^{2-} (stability) can be evaluated by the degree of polymerization (Q^3/Q^2 ratio, Q^i represents the tetrahedral structure unit with different number of bridging oxygen, *i*) of network structure and the excess free energy (or activity coefficient) of MS (M = Ca or Mn), respectively.[12–17,32] Succeeding this methodology, the sulfide capacity of the MnO-SiO_2-Al_2O_3-Ce_2O_3 system can be understood based on the structure analysis using micro-Raman spectroscopy.

The Raman spectra of the MnO-SiO_2-Al_2O_3 ternary system are shown in Figure 8 at different M/S ratios (2.2 and 1.0) in order to preliminarily confirm the influence of the basicity on the structure of Mn-aluminosilicate system. The Raman bands in the present ternary system can be divided into two major sections, which are 400 to 800 and 800 to 1200 cm^{-1} range. Several authors reported that the Raman band between 400 and 600 cm^{-1} has been associated with the bending motion of bridging oxygen in T-O-T (T = Si or Al) linkages.[33–35] Thus, the band at about 500 cm^{-1} can be a characteristic band of high silica, viz. highly polymerized, system.

Okuno *et al.*[36] recently observed that the band at 600 to 700 cm^{-1} in quenched aluminosilicate glasses is assigned to the symmetric stretching vibrations of $[AlO_6]$ species. Moreover, we recently found that Raman scattering at 700 to 850 cm^{-1} in the low silica calcium aluminosilicate melts could be assigned as $[AlO_4]$-units with different NBOs.[37] Because the Al-O bond strength in $[AlO_6]$-unit is weaker than that in $[AlO_4]$-unit,[38] the Raman scattering of $[AlO_6]$-unit should be occurred at lower wavenumbers than that of $[AlO_4]$-units. Therefore, we assumed that the band at about 600 cm^{-1} represents the $[AlO_6]$-units in the present system.

The Raman scattering at 800 to 1200 cm^{-1} is assigned to the asymmetric Si-O stretching vibration and shifts to the higher wavenumber as M/S ratio decreases, indicating that the relative fraction of Q^3_{Si} unit increases by increasing the silica content.[14–17,34–36] From the change of this asymmetric Si-O stretching vibration band as a function of melt composition, it can be concluded that the degree of polymerization (Q^3_{Si}/Q^2_{Si}) increases with increasing content of SiO_2 in conjunction with a consumption of free oxygen ions. Consequently, sulfide capacity of the melts decreases as indicated in Figures 4 and 8.

The Raman spectra of the MnO-SiO_2-Al_2O_3-Ce_2O_3 systems (M/S = 2.2 and 1.0) are shown in Figures 9 and 10 in order to understand the relationship between the structural change and the variation of sulfide capacity of the oxide melts. From the Raman spectra shown in Figures 9 and 10, it is commonly found that the Raman band for the Si-O asymmetric stretching vibration between 800 and 1150 cm^{-1} very slightly shifts to the lower wavenumbers by increasing the content of Ce_2O_3, indicating that there is no considerable change in the environment of silicate units by the incorporation of Ce^{3+} ions. In the Raman spectra of the M/S = 2.2 system shown in Figure 9, there is a significant increase in the relative intensity of the scattering band at about 600 cm^{-1} with increasing content of Ce_2O_3. This means that there are dramatic changes in the aluminosilicate structure, even though the alumina and silica content does not significantly change with increasing content of Ce_2O_3. In the present study, it is reasonable that the increase in the relative intensity of Raman band at 600 cm^{-1} is due to the $[AlO_6]$-unit as mentioned by Okuno *et al.*,[39] because of the strong attraction between Al_2O_3 and Ce_2O_3 in the present system.[26–29] However, a significant increase in the relative intensity of $[AlO_6]$-unit band at about 600 cm^{-1} due to Ce^{3+} addition was not observed in the less basic melts, viz. M/S = 1.0 system as shown in Figure 10. These

complicated phenomena can be explained by considering the amphoteric behavior of alumina in the aluminosilicate melts as follows.

Generally, the Al-O bond coordination is tetrahedral, representing the network forming role of Al_2O_3 under conditions of plenty of charge balancing cations, *i.e.*, in the highly basic (less silica) melts. However, the Al-O bond has an octahedral coordination, representing the network modifying role of Al_2O_3 under conditions of deficiency of charge balancing cations, *i.e.*, in the less basic (high silica) melts.[30,31,39] Before adding Ce_2O_3, the concentration of $[AlO_6]$-unit in the M/S = 0.3-1.0 systems are larger than that in the M/S = 2.2 system. Thus, Ce^{3+} ions added in medium (M/S = 1.0) and high silica (M/S = 0.3) melts instantly interact with large amounts of (pre-existing) $[AlO_6]$-units to form more stable $[(Al,Ce)O_6]$-unit (Eq. [7]) as schematically shown in Figure 11(a). Therefore, the structure of aluminosilicate melts was not significantly disturbed by addition of Ce_2O_3, resulting in the insensitive dependency of sulfide capacity of the melts on the content of Ce_2O_3 as shown in Figure 5. The sulfide capacities of these systems are mainly affected by a dilution of MnO as discussed in Section III–B.

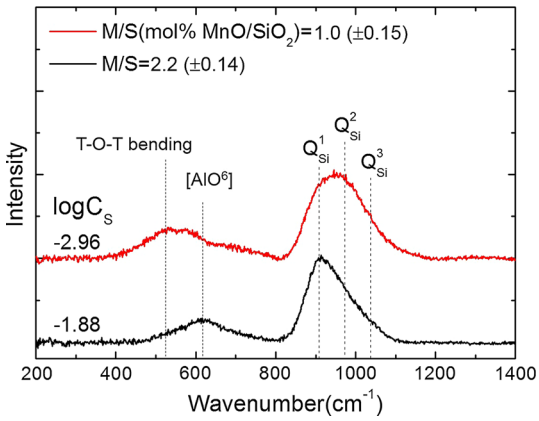

Fig. 8—Effect of MnO/SiO_2 ratio on the Raman scattering band of the quenched $MnO\text{-}SiO_2\text{-}Al_2O_3$ system.

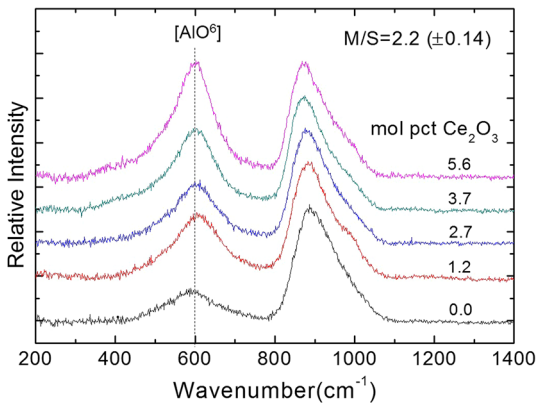

Fig. 9—Effect of Ce_2O_3 addition on the Raman scattering band of the $MnO\text{-}SiO_2\text{-}Al_2O_3\text{-}Ce_2O_3$ system (MnO/SiO_2 = 2.2).

On the other hand, in the low silica system (M/S = 2.2), relatively large amounts of (pre-existing) $[(Al,Mn_{0.5})O_4]$-units should be converted to the $[(Al,Ce)O_6]$-unit with consumption of free oxygen by addition of Ce^{3+} ions (Eq. [7]) as shown in Figure 11(b), resulting in a decreases in sulfide capacity. However, the sulfide capacity increases by addition of Ce_2O_3 greater than about 4 mol pct because the excess Ce^{3+} and free Mn^{2+} cations contribute to the stabilization of S^{2-} ions. This tendency was not observed in

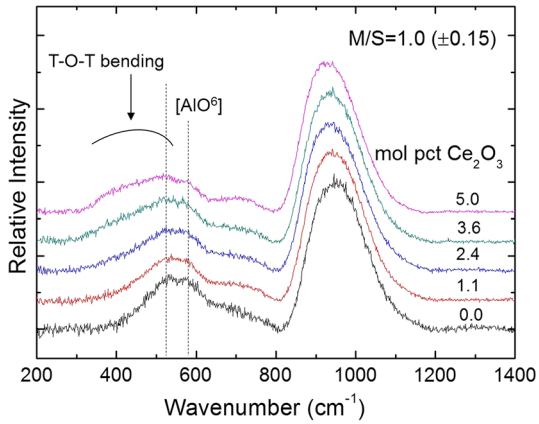

Fig. 10—Effect of Ce_2O_3 addition on the Raman scattering band of the $MnO\text{-}SiO_2\text{-}Al_2O_3\text{-}Ce_2O_3$ system (MnO/SiO_2 = 1.0).

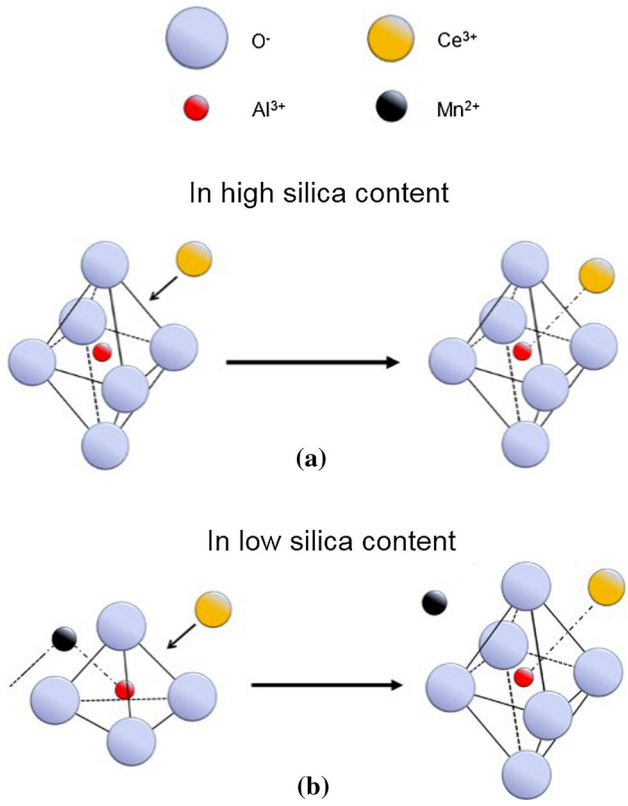

Fig. 11—Schematics of the structural changes by addition of Ce^{3+} to the Mn-aluminosilicate melts (*a*) at high SiO_2 (low MnO/SiO_2) system and (*b*) at low SiO_2 (high MnO/SiO_2) system.

the M/S = 0.3-1.0 systems because the cations (Ce^{3+} and Mn^{2+}) are still not free from a charge balancing role with large amounts of silicate and/or aluminate anions within the present experimental compositions.

In summary, the sulfide capacity of Mn-aluminosilicate melts decreases by addition of Ce_2O_3 and this tendency is more significant in the highly basic (high MnO/SiO_2) melts, which originated from the following three thermodynamic and structural factors. First, the activity of basic oxide, MnO in the oxide melts decreases by addition of Ce_2O_3 and the activity decreasing rate is more dominant in the high MnO/SiO_2 melts, resulting in a decrease in the basicity of the melts. Second, the free oxygen is consumed in the structure modification from $[(Al,Mn_{0.5})O_4]$- to $[(Al,Ce)O_6]$-unit (Eq. [7]) by addition of Ce_2O_3, which is significantly occurred in the high MnO/SiO_2 melts, resulting in a decrease in the basicity of the melts. Finally, when the Ce^{3+} content is greater than critical value (approx. 4 mol pct in the present system) in the high MnO/SiO_2 (=2.2) melts, excess Ce^{3+} and Mn^{2+} ions competitively react with S^{2-} ions, resulting in an increase of sulfide capacity due to a decrease in the activity coefficient of S^{2-} ions, $f_{S^{2-}}$ in the melts.

IV. CONCLUSIONS

We measured the sulfide capacity of the MnO-SiO_2-Al_2O_3-Ce_2O_3 quaternary system by gas-slag equilibration method at 1873 K (1600 °C), and the structural analysis was also carried out using micro-Raman spectroscopic method to understand the role of Ce_2O_3 in the sulfur dissolution behavior in the present oxide system because none of thermodynamic information (activity of each component, phase equilibria, *etc.*) of the MnO-SiO_2-Al_2O_3-Ce_2O_3 system is available. The following conclusions could be made.

1. From the XPS analysis of the quenched glass samples, it was confirmed that Ce is stable as Ce_2O_3 (Ce^{3+}) rather than CeO_2 (Ce^{4+}) in the MnO-SiO_2-Al_2O_3-CeO_x system under the present experimental conditions.
2. The influence of Ce_2O_3 on the sulfide capacity of the MnO-SiO_2-Al_2O_3-Ce_2O_3 system exhibited a different tendency according to the MnO/SiO_2 (=M/S) ratio. The sulfide capacity of the oxide melts with highly basic composition, *i.e.*, M/S = 2.2, decreased with increasing content of Ce_2O_3 to approx. 4 mol pct, beyond which the sulfide capacity increased. The sulfide capacity continuously decreased as the Ce_2O_3 was added to the Mn-aluminosilicate melts in the less basic system, *i.e.*, M/S = 1.0, whereas it was hardly affected by Ce_2O_3 in the relatively acidic (high silica) composition, *i.e.*, M/S = 0.3.
3. There was a significant increase in the relative intensity of the Raman scattering band at about 600 cm^{-1} with increasing content of Ce_2O_3 in the high MnO/SiO_2 system, which originated from the transition from $[AlO_4]$-unit balanced by $0.5Mn^{2+}$, *i.e.*, $[(Al,Mn_{0.5})O_4]$-tetrahedron to the Ce^{3+} incorporated $[AlO_6]$-unit, *i.e.*, $[(Al,Ce)O_6]$-octahedron because of the strong attraction between Al_2O_3 and Ce_2O_3 in the present system. However, this structure modification reaction was not observed in the less basic melts, viz. M/S = 1.0 system.
4. The changes in the sulfide capacity of the Mn-aluminosilicate melts by addition of Ce_2O_3 could be explained by the following factors. First, the activity of MnO in the melts decreased by addition of Ce_2O_3 and the activity decreasing rate was more dominant in the high MnO/SiO_2 melts, resulting in a decrease in the basicity of the melts. Second, the free oxygen was consumed in the structure modification reaction from $[(Al,Mn_{0.5})O_4]$- to $[(Al,Ce)O_6]$-unit by addition of Ce_2O_3, which was significantly occurred in the high MnO/SiO_2 melts, resulting in a decrease in the basicity of the melts. Finally, when the Ce^{3+} content is greater than critical value (approx. 4 mol pct in the present system) in the high MnO/SiO_2 (=2.2) melts, excess Ce^{3+} and Mn^{2+} ions competitively react with S^{2-} ions, resulting in an increase of sulfide capacity due to a decrease in the activity coefficient of S^{2-} ions in the melts.

ACKNOWLEDGMENTS

This research was supported by the Basic Science Research Program through the National Research Foundation of Korea (NRF) funded by the Ministry of Education (Grant Number NRF-2012R1A1A2041774). Furthermore, the authors express the appreciation to Professor KAZUKI MORITA, The University of Tokyo, Japan, for a fruitful discussion in regard of the interaction between Ce_2O_3 and Al_2O_3 in oxide melts.

REFERENCES

1. S.T. Kim, S.H. Jeon, I.S. Lee, and Y.S. Park: *Corros. Sci.*, 2010, vol. 52, pp. 1897–1904.
2. S.H. Jeon, S.T. Kim, I.S. Lee, and Y.S. Park: *Corros. Sci.*, 2010, vol. 52, pp. 3537–47.
3. S.K. Kwon, Y.M. Kong, and J.H. Park: *Met. Mater. Int.*, 2014, vol. 20, pp. 959–66.
4. S.K. Kwon, J.S. Park, and J.H. Park: *ISIJ Int.*, 2015, vol. 55, pp. 2589–96.
5. R.A. Sharma and F.D. Richardson: *Trans. Metall. Soc. AIME*, 1965, vol. 233, pp. 1586–92.
6. M.M. Nzotta: *Scand. J. Metall.*, 1997, vol. 26, pp. 169–77.
7. Y.B. Kang and A.D. Pelton: *Metall. Mater. Trans. B*, 2009, vol. 40B, pp. 979–94.
8. D.H. Woo, Y.B. Kang, and H.G. Lee: *Metall. Mater. Trans. B*, 2002, vol. 33B, pp. 915–20.
9. H. Ohta and H. Suito: *Metall. Mater. Trans. B*, 1996, vol. 27B, pp. 263–70.
10. T. Fujisawa and H. Sakao: *Tetsu-to-Hagane*, 1977, vol. 63, pp. 1504–11.
11. N.M. Anacleto, H.G. Lee, and P.C. Hayes: *ISIJ Int.*, 1993, vol. 33, pp. 549–55.
12. G.H. Park, Y.B. Kang, and J.H. Park: *ISIJ Int.*, 2011, vol. 51, pp. 1375–82.
13. J.H. Park and G.H. Park: *ISIJ Int.*, 2012, vol. 52, pp. 764–69.
14. J.H. Park: *Steel Res. Int.*, 2013, vol. 84, pp. 664–69.
15. J.H. Park: *J. Non-Cryst. Solids*, 2012, vol. 358, pp. 3096–3102.

16. J.H. Park, K.Y. Ko, and T.S. Kim: *Metall. Mater. Trans. B*, 2015, vol. 46B, pp. 741–48.
17. J.H. Park: *ISIJ Int.*, 2012, vol. 52, pp. 1627–36.
18. E.J. Preisler, O.J. Marsh, R.A. Beach, and T.C. McGill: *J. Vac. Sci. Technol. B*, 2001, vol. 19, pp. 1611–18.
19. J.A-Rivera, D.A.R. Carvajal, M. del C. A-Enriquez, M.B.M-Martinez, E. Alvarez, R. L-Morales, G. C. Diaz, A. de Leon, and M. E. Zayas: *J. Am. Ceram. Soc.*, 2014, vol. 97, pp. 3494–500.
20. M. Sekita, A. Fujimori, A. Makishima, and T. Shimohira: *J. Non-Cryst. Solids*, 1985, vol. 76, pp. 399–407.
21. A. Makishima, M. Kobayashi, and T. Shimohira: *Commun. Am. Ceram. Soc.*, 1982, vol. 65, C-210-C-211.
22. C.J.B. Finchan and F.D. Richardson: *Proc. R. Soc. London A*, 1954, vol. 223, pp. 40–62.
23. R. G. Ward: An Introduction to the Physical Chemistry of Iron and Steelmaking, Edward Arnold, 1962.
24. Y.B. Kang and J.H. Park: *Metall. Mater. Trans. B*, 2011, vol. 42B, pp. 1211–17.
25. A. Vahed and D.A.R. Kay: *Metall. Trans. B*, 1976, vol. 7B, pp. 375–83.
26. S.L. Lin, C.S. Hwang, and J.F. Lee: *Jpn. J. Appl. Phys.*, 1996, vol. 35, pp. 3975–83.
27. P. Wu and A.D. Pelton: *J. Alloys Compd.*, 1992, vol. 179, pp. 259–87.
28. S. Ueda, K. Morita, and N. Sano: *ISIJ Int.*, 1998, vol. 38, pp. 1292–96.
29. R. Kitano, M. Ishii and K. Morita: *Proc. of 6th Asia Steel Int. Conf.*, 2015, pp. 40-41.
30. J.H. Park, D.J. Min, and H.S. Song: *Metall. Mater. Trans. B*, 2004, vol. 35B, pp. 269–75.
31. B.O. Mysen, D. Virgo, and C.M. Scarfe: *Am. Mineral.*, 1980, vol. 65, pp. 690–710.
32. J.H. Park: *Met. Mater. Int.*, 2013, vol. 19, pp. 557–84.
33. K. Chah, B. Boizot, B Reynard, D. Ghaleb, and G. Petite: *Nucl. Instrum. Meth. B*, 2002, vol. 191, pp. 337–41.
34. F. Seifert, B.O. Mysen, and D. Virgo: *Am. Mineral.*, 1982, vol. 67, pp. 696–718.
35. P. McMillan, B. Piriou, and A. Navrotsky: *Geochim. Cosmochim. Acta*, 1982, vol. 46, pp. 2021–37.
36. M. Okuno, N. Zotov, M. Schmucker, and H. Schneider: *J. Non-Cryst. Solids*, 2005, vol. 351, pp. 1032–38.
37. T.S. Kim and J.H. Park: *ISIJ Int.*, 2014, vol. 54, pp. 2031–38.
38. J.H. Park, D.J. Min, and H.S. Song: *ISIJ Int.*, 2002, vol. 42, pp. 38–43.
39. B.O. Mysen and P. Richet: *Silicate Glasses and Melts: Properties and Structure*, Elsevier, Amsterdam, 2005.